Halofuginone suppresses the lung metastasis of chemically induced hepatocellular carcinoma in rats through MMP inhibition

Danièle Taras[*,†], *Jean-Frédéric Blanc*[*,†], *Anne Rullier*[*,†], *Nathalie Dugot-Senant*[†], *Ingrid Laurendeau*[‡], *Ivan Bièche*[‡], *Mark Pines*[§] *and Jean Rosenbaum*[*,†]

*INSERM, E362, Bordeaux, F-33076 France; Université Victor Segalen Bordeaux 2, Bordeaux, F-33076 France. [†]IFR 66, Bordeaux, F-33076 France. [‡]Université Paris 5, UPRES EA 3618-Laboratoire de Génétique Moléculaire, Paris, F-75006 France. [§]Institute of Animal Science, the Volcani Center, Bet Dagan, Israel.

Abstract

Halofuginone, an inhibitor of collagen synthesis, appears to be a promising antitumoral drug in preclinical studies. We used a relevant rat model of autochthonous, chemically induced, spontaneously metastasizing hepatocellular carcinoma (HCC) to test the efficacy of halofuginone on tumor progression and matrix metalloproteinase (MMP) expression. Following sequential administration of diethylnitrosamine and *N*-nitrosomorpholine for 14 weeks, all animals developed HCC and then received halofuginone or its solvent for 10 weeks. The final number of liver tumors was lower in the halofuginone group than in the solvent group (57.2 ± 4.6 *vs* 68 ± 5.0; $P < .01$). The percentage of the lung surface infiltrated by metastasis was much smaller in the halofuginone group (0.3 ± 0.2%) than in the solvent group (13.5 ± 10.1%; $P < .02$). MMP-9 activity was decreased in the halofuginone group by 89% and 63% in non-neoplastic parts of the liver and tumor, respectively. The percentage of active MMP-2 was reduced by 90% in non-neoplastic parts of the liver and by 61% in tumors. This was likely subsequent to a decreased expression of both MMP-14 and tissue inhibitor of matrix metalloproteinase-2, which are required for pro–MMP-2 activation. These results, obtained from a clinically relevant model, further suggest the potential benefit of halofuginone in HCC.

Neoplasia (2006) **8,** 312–318

Keywords: Hepatocellular carcinoma, metastasis, metalloproteinase, TIMP-2, halofuginone.

Introduction

Hepatocellular carcinoma (HCC) is one of the most common cancers [1], and its prognosis is still very poor because it is associated, in most cases, with chronic liver disease and has a propensity to invade the liver and to metastasize. Curative surgery or liver transplantation is rarely possible and often leads to tumor recurrence [2]. Even if palliative treatments such as radiofrequency ablation have shown some success [3], there is still a need for new treatments, especially for advanced tumors.

Halofuginone is an analog of a low-molecular-weight quinazolinone alkaloid isolated from the plant *Dichroa febrifuga*. It is widely used as a coccidiostat in chickens and turkeys, and is a potent inhibitor of collagen type α1 (I) gene expression and extracellular matrix (ECM) deposition [4]. This effect on ECM deposition has led to the demonstration that halofuginone has strong antifibrotic properties in several organs, such as the liver [5,6], skin [7], or lung [8].

Halofuginone also inhibits tumor progression. This was shown in models of grafted tumor cells of bladder carcinoma [9], pheochromocytoma [10], prostate cancer [11], sarcoma [12], or Wilms tumor [13], as well as in a model of chemically induced bladder cancer [9]. The antitumor effect of halofuginone was attributed to its action on several critical steps in primary tumor progression, such as angiogenesis [9,14], stromal support [9], and cell proliferation [9]. Moreover, halofuginone also suppressed the transcription of the *MMP-2* gene [10,14,15], which is associated with a marked decrease in ECM invasion *in vitro* and lung colonization by bladder carcinoma cells [15]. Very recently, it was shown that halofuginone could suppress the growth of HCC in a xenograft model [16].

The aim of the present study was to test whether halofuginone would have beneficial effects on tumor progression and metastasis development in the clinically relevant setting of established HCC in rats with chemically induced HCC.

Materials and Methods

Animals

Five-week-old male Fischer F344 rats were obtained from Charles River (St. Aubin les Elbeuf, France) and were housed

Abbreviations: HCC, hepatocellular carcinoma; ECM, extracellular matrix; MMP, metalloproteinase; TIMP-2, tissue inhibitor of matrix metalloproteinase-2

Address all correspondence to: Jean Rosenbaum, GREF, INSERM E362, Université Victor Segalen, Bordeaux 2, Bordeaux, France. E-mail: jean.rosenbaum@gref.u-bordeaux2.fr

DOI 10.1593/neo.05796

five per cage in an air-conditioned room at 22°C and 55% humidity, with a 12-hour light/dark cycle for 1 week before the beginning of the experiments. Food and tap water were available *ad libitum*. The experiments were conducted according to institutional and national guidelines for the care and use of laboratory animals.

Experimental Protocol

HCCs were induced essentially as described by Futakuchi et al. [17], with slight modifications. Rats were given a single intraperitoneal injection of diethylnitrosamine (Sigma Aldrich, St. Quentin Fallavier, France) at a dose of 100 mg/kg body weight as initiator of liver carcinogenesis. Then, they received 80 ppm of *N*-nitrosomorpholine (Tokyo Kasei, Tokyo, Japan) in drinking water for 14 weeks.

Thirty-five animals were used in this study. Twenty-five animals were submitted to the carcinogenesis protocol described above. On week 14, they were further divided into three groups. Group 1 included five animals that were sacrificed to check the presence of histologically confirmed HCC. Animals in groups 2 and 3 ($n = 10$ per group) received daily intraperitoneal injections of halofuginone (Collgard Biopharmaceuticals Ltd., Petach Tikva, Israel) at a dose of 100 μg/kg body weight in 0.9% NaCl or saline only, respectively, for 10 weeks.

Groups 4 and 5 were control groups of five animals each that did not receive any carcinogen but received halofuginone alone or solvent alone, respectively, from week 14 onward.

At the end of the experiment (week 24), surviving animals (see Results section) were sacrificed under ketamine anesthesia. Two hours prior to sacrifice, animals received an intraperitoneal injection of 100 mg/kg bromodeoxyuridine (BrdU). The body, liver, spleen, and lungs were weighed, and an autopsy was performed. Liver nodules or tumors visible at the surface of the liver and greater than 3 mm in diameter were counted and measured. Multiple samples were taken from tumors and from the apparently non-neoplastic portion of the liver.

The lungs were separated into the right lobe and the left lobe. Six plane sections of each lobe were made at 0.4-cm intervals.

Histology and Immunohistochemistry

Formalin-fixed paraffin-embedded samples were sectioned at 4 μm and routinely stained with hematoxylin and eosin.

BrdU staining was performed as previously described [18]. Stained hepatocyte nuclei were counted in 10 random fields using ×20 objective. Blood vessels were immunostained using an antibody to von Willebrand factor (Abcam, Cambridge, UK).

Quantification of Lung Infiltration with Metastasis

Lung sections stained with hematoxylin and eosin were photographed with a digital camera (EDAS 120; Kodak, Rochester, NY). The total area of the section was measured with ImageJ software (http://rsb.info.nih.gov/ij). The sections were examined under a Zeiss Axioplan 2 microscope (Carl Zeiss Microscopy, Jena, Germany). Images were acquired with the Zeiss MC 80 DX AxioCam (Carl Zeiss Vision, Hallbergmoos, Germany) by means of the Axiovision image processing and analysis system (Carl Zeiss Vision). The surface area of metastatic nodules was obtained using a computerized image analysis system (KS300; Carl Zeiss Vision). We could thus calculate for each section the percentage of the section occupied by metastasis. The mean percentage ± SD of all sections for a given animal was calculated and used as an indicator of metastasis burden.

Gelatin Zymography

Gelatin zymography was performed essentially as described by Musso et al. [19]. Sixteen-micrometer cryostat sections were solubilized in 25 μl of 10% glycerol and 1% sodium dodecyl sulfate (SDS) at room temperature for 15 minutes. Protein concentration was estimated from A_{280} readings.

Twenty microliters of samples normalized for protein concentration was electrophoresed on a 10% SDS polyacrylamide gel containing 1 mg/ml gelatin. After washing with 2.5% Triton X-100, the gel was incubated overnight at 37°C in 50 mM Tris–HCl, pH 8, supplemented with 5 mM $CaCl_2$. Gels were finally stained for 15 minutes in 40% methanol/10% acetic acid containing 0.25% Coomassie brilliant blue and destained in H_2O. Proteolytic activity was detected as a white zone in a dark blue field.

For quantitative purposes, gel pictures were acquired with a digital camera as above, and the intensity of proteolytic bands was measured using the Kodak 1D 3.0 USB software. Results were expressed in arbitrary units.

Real-Time Reverse Transcription Polymerase Chain Reaction (RT-PCR)

Total RNA was extracted from liver samples following grinding in liquid nitrogen, using the RNeasy Mini kit (Qiagen, Courtaboeuf, France). Transcripts of MMP-2, MMP-9, MMP-14, and tissue inhibitor of matrix metalloproteinase-2 (TIMP-2) were quantified by a method of quantitative RT-PCR, which has previously been described in detail [20]. Each sample was normalized based on its expression of the *RPLP0* gene (also known as 36B4, encoding acidic ribosomal phosphoprotein P0).

Statistical Analysis

All data were expressed as mean ± SD. Mann-Whitney test and one-way analysis of variance (ANOVA) were performed using the Statcrunch package (www.statcrunch.com). When required, post hoc Tukey's test was applied following ANOVA (www.cvgs.k12.va.us/DIGSTATS/Imain.html). Survival data were analyzed with log-rank test. Results were considered to be significant when $P < .05$.

Results

In preliminary experiments, we found that every animal that submitted to this protocol developed histologically confirmed HCC by the 14th week of treatment (Figure 1*A*). These tu-

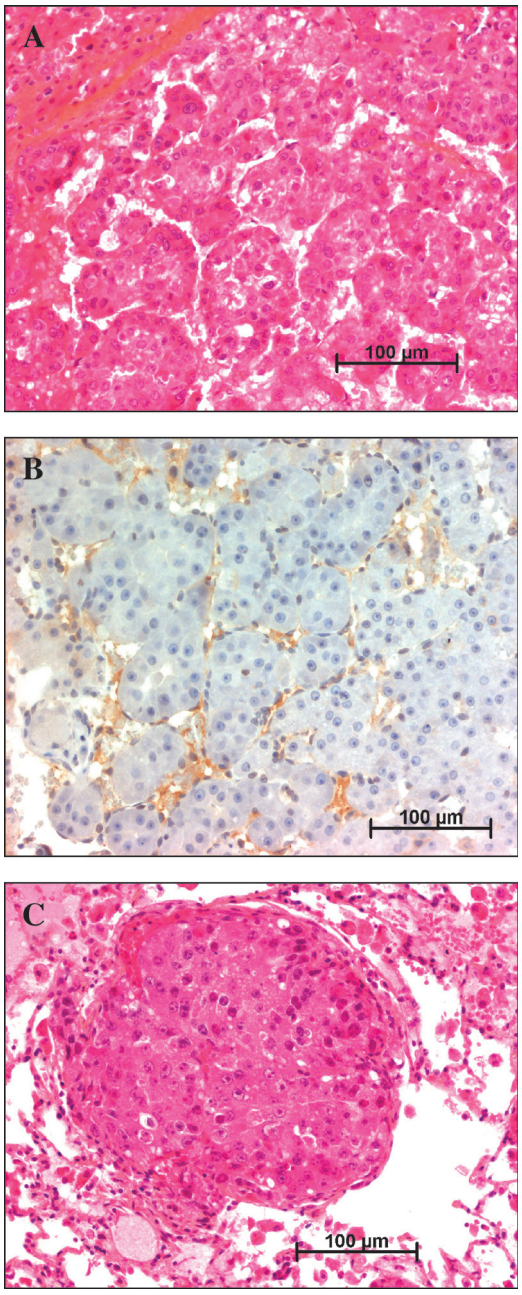

Figure 1. *Histology of tumors. (A) Liver tumor from a solvent-treated animal, stained with hematoxylin–eosin–saffron. (B) Immunostaining for von Willebrand factor in a liver tumor showing intense staining. (C) Lung metastasis from a solvent-treated animal, stained with hematoxylin–eosin–saffron.*

mors were highly vascularized, as shown by von Willebrand factor immunostaining (Figure 1*B*). After week 14 and until the death of the animals, the tumors increased in size and number. On week 24, every surviving animal had lung metastatic nodules (Figure 1*C*).

Vital Parameters

From week 14 onward, control animals kept gaining weight steadily, whereas carcinogen-treated animals did not. Halofuginone treatment had no adverse effects on the weight curve in either control or carcinogen-treated animals (Figure 2*A*). At the time of sacrifice, the mean body weight was marginally, but not significantly, higher in halofuginone-treated rats compared to controls (302.0 ± 9.0 *vs* 290.0 ± 15.6 g).

No death occurred in animals that did not receive carcinogens. Halofuginone treatment delayed the onset of mortality in animals bearing HCCs because the first death occurred on week 7 posttreatment *versus* week 4 in controls. The final survival rate on week 24 reached 50% and 40% in halofuginone and control groups, respectively. The difference was not significant (Figure 2*B*).

Liver Tumors

At the time of sacrifice, the livers of all animals were infiltrated with a large number of tumors, making the precise assessment of tumor mass impossible. We thus used two indirect estimates. First, we quantified the number of nodules (with a diameter > 3 mm) that were detectable at the surface of the liver. In four surviving solvent-treated animals, there were 68.0 ± 5.0 nodules, whereas there were only 57.2 ± 4.6 nodules in five remaining halofuginone-treated animals ($P < .01$, Mann-Whitney test; Figure 3*A*). Small nodules may

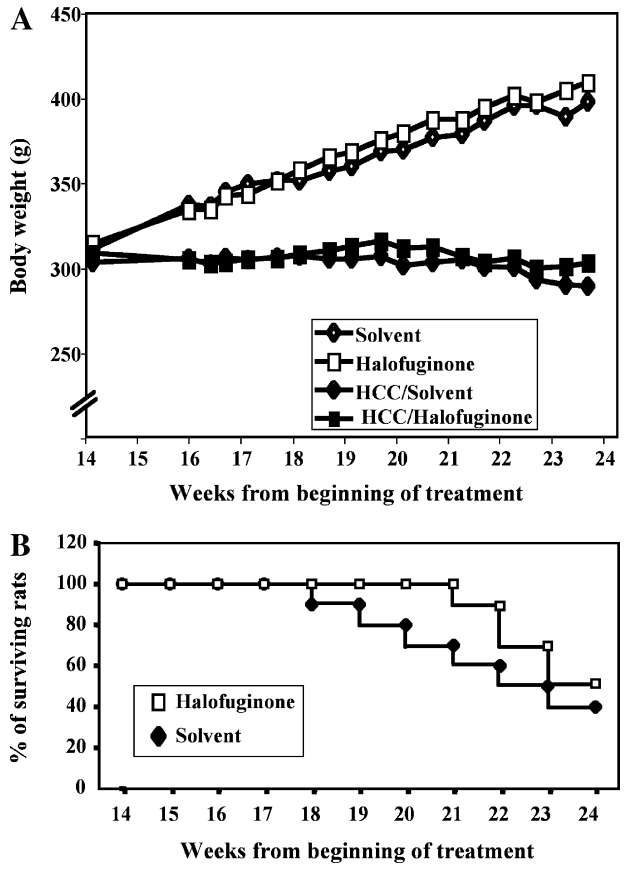

Figure 2. *Vital parameters. (A) Growth curve of animals. The curves begin on week 14, the time at which all animals bear HCCs and treatment with halofuginone or its solvent begins. Open symbols refer to animals that did not receive any carcinogens, whereas closed symbols refer to carcinogen-treated HCC-bearing animals. Standard deviations are not represented for the sake of clarity and were always < 12% of the mean. (B) Survival curve. This was also plotted starting from the beginning of treatment on week 14. The graph shows data only for HCC-bearing animals because there was no death in animals that did not receive carcinogens.*

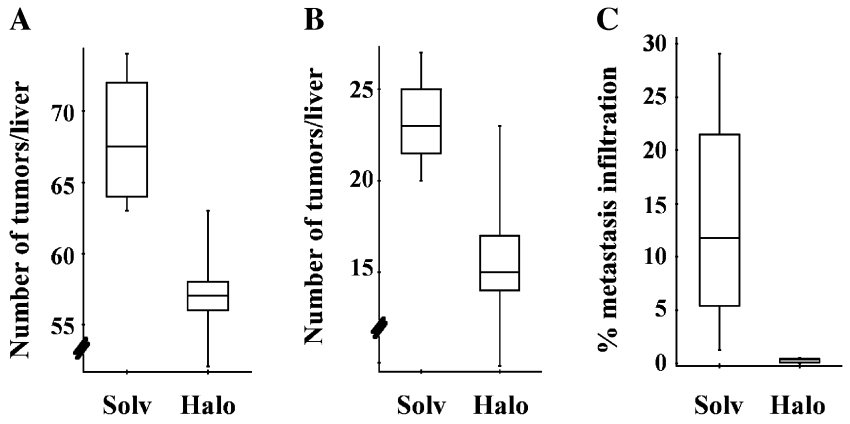

Figure 3. *Tumor burden. Tumor burden was evaluated at the time of sacrifice of surviving animals (solvent group, n = 4; halofuginone group, n = 5). (A and B) Box-and-whiskers plot of the number of nodules > 3 mm in diameter or > 6 mm, respectively. The top and bottom of each box represents the 75th and 25th percentiles, respectively. Whiskers represent the range, and the line in the box represents the median value of the distribution. The differences between the solvent and halofuginone groups were statistically significant in both cases using the Mann-Whitney test (P < .01 and P < .02, respectively). (C) The percentage of lung section surface infiltrated by metastasis was quantified as described in Materials and Methods section. The difference between groups was highly significant (P < .02; Mann-Whitney test).*

include actual HCCs with prenoplastic lesions. However, in our preliminary experiments, we found that nodules larger than 6 mm in diameter on week 24 were always HCCs. When we counted only nodules > 6 mm in diameter, the average number was 23.3 ± 2.9 in control animals and only 16.8 ± 4.0 in animals treated with halofuginone ($P < .02$; Figure 3*B*). As a second estimate of tumor mass, we measured liver weight and the liver weight/body weight ratio. Both liver weight (30.6 ± 1.8 *vs* 31.9 ± 2.5 g) and liver weight/body weight ratio (10.1 ± 0.3% *vs* 11.0 ± 0.8%) were lower in halofuginone-treated animals than in solvent-treated animals, although the differences were not statistically significant.

No gross differences were seen on histologic examination of liver tumors from both groups of animals. There was also no difference in vascularity, as assessed by von Willebrand factor staining (data not shown). Cell proliferation was measured with BrdU staining, and no significant difference was seen between the solvent group (29.5 ± 11.3 positive hepatocytes per field) and the halofuginone group (20.0 ± 11.2 positive hepatocytes per field) (Figure 4).

Lung Metastasis

The extent of lung metastasis was significantly different between the two groups. Although metastasis was detectable in every animal, the percentage of the lung surface section occupied by metastasis was 13.5 ± 10.1% in the control group (range, 1.3–29.1%) *versus* only 0.30 ± 0.24% (range, 0.01–0.5%) in halofuginone-treated animals ($P < .02$, Mann-Whitney test; Figure 3*C*).

MMP Expression and Activity

The enzymatic activity of gelatinases was measured on solubilized frozen sections taken from experimental animals. These activities were measured separately in tumors and in macroscopically nontumoral areas. For comparative purposes, we used tumors of similar sizes in the solvent and halofuginone groups (about 5 mm in diameter). Samples from control and halofuginone-treated animals were compared on the same gels. MMP-2 or MMP-9 activities were below the detection threshold in animals that did not receive carcinogens (not shown). Figure 5 shows representative gels, and Table 1 summarizes data concerning MMP-9 and MMP-2 in tumor-bearing animals.

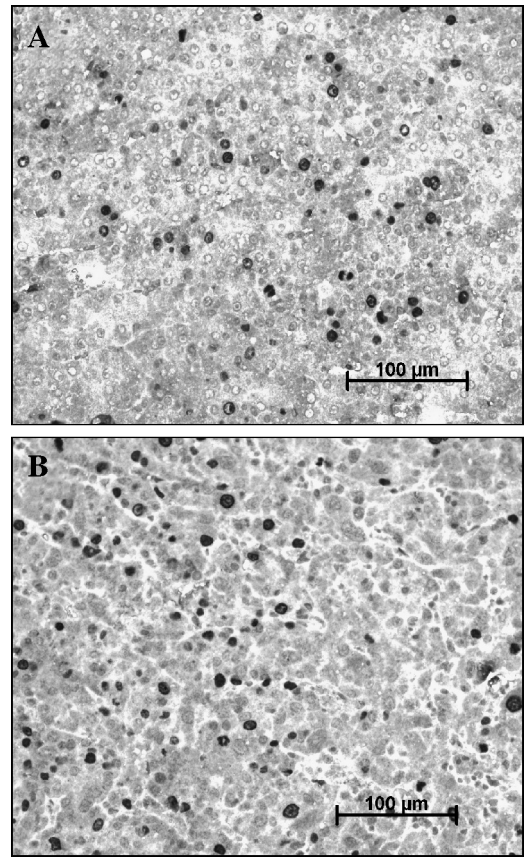

Figure 4. *Immunostaining for BrdU. Liver sections from solvent-treated (A) or halofuginone-treated (B) animals were immunostained for BrdU. Positive nuclei appear dark. No quantitative differences were seen between the two groups.*

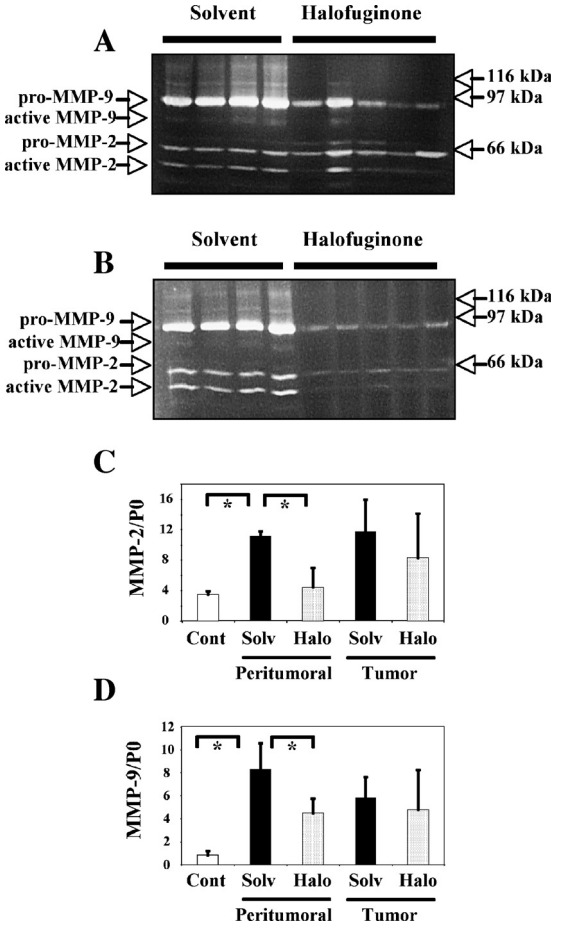

Figure 5. *Expression of MMP-2 and MMP-9. (A and B) Gelatin zymography. Tissue samples were obtained from control animals (n = 4) or halofuginone-treated animals (n = 5). MMP activity was measured in gelatin-containing gels, either in tumors (A) or in corresponding non-neoplastic parts of the liver from the same animals (B). The experiment was repeated several times with identical results. Data quantification is shown in Table 1. (C and D) Expression of transcripts of MMP-2 and MMP-9. Transcripts of MMP-2 and MMP-9 were assayed by quantitative PCR, and results were normalized according to the level of the P0 gene. Results are shown as mean ± SD. MMP-2 is shown in (C) and MMP-9 is shown in (D). "Cont" refers to control animals that did not receive any carcinogens. "Solv" and "Halo" refer to animals bearing HCC that were treated with solvent or halofuginone, respectively. Measurements were made either in non-neoplastic parts of the liver or within tumors, as indicated. One-way analysis of variance showed that overall results differed significantly between groups (P < .01 for MMP-2 and P < .003 for MMP-9). Asterisks indicate significant differences between individual groups by post hoc Tukey's test (P < .01).*

A band migrating at 95 kDa and corresponding to pro–MMP-9 was detected in every experimental sample. The mean intensity of this band was significantly decreased in halofuginone-treated animals, both in tumors (Figure 5*A*) and in non-neoplastic parts of the liver (Figure 5*B*), compared with solvent-treated animals. Active MMP-9 was barely detectable in animals receiving the solvent and was undetectable in halofuginone-treated animals.

Regarding MMP-2, a band migrating at 66 kDa corresponding to pro–MMP-2 was detected in every sample, whereas a 62-kDa band corresponding to active MMP-2 was seen in only some of them. The mean amount of MMP-2 (pro + active) was significantly decreased in non-neoplastic parts of the liver from halofuginone-treated animals (Figure 4*B*), but was similar in tumors from both groups of animals (Figure 5*A*). However, the percentage of active MMP-2 was much lower in halofuginone-treated animals, in tumors (39% of the values of solvent-treated animals) (Figure 5*A*), and in non-neoplastic parts of the liver (10% of the values of solvent-treated animals; $P < .01$ in both cases) (Figure 5*B*). Specifically, active MMP-2 was detected in non-neoplastic parts of the liver of every solvent-treated animal, but only in one from the halofuginone group.

A shown in Figure 5, *C* and *D*, analysis of MMP-2 and MMP-9 transcripts by quantitative RT-PCR correlated well with zymography experiments, although the decrease in MMP-9 transcripts in non-neoplastic parts of the liver failed to reach statistical significance.

Pro–MMP-2 activation is carried out at the cell surface by a complex composed of MMP-14 (or MT1-MMP) and TIMP-2 [21,22]. We thus measured the expression of these two components using quantitative RT-PCR. As shown in Figure 6, the expression of MMP-14, expressed as MMP-14/P0 ratio, was significantly reduced by halofuginone treatment in tumors (from 5.20 ± 1.59 to 2.47 ± 1.07) and in non-neoplastic parts of the liver (from 6.28 ± 0.29 to 2.63 ± 1.51) compared with the solvent. The same was true for TIMP-2, with a decrease from 11.21 ± 4.74 to 5.71 ± 4.50 in tumors and from 16.20 ± 3.25 to 3.72 ± 1.64 in non-neoplastic parts of the liver.

Discussion

The results of this study indicate that halofuginone had limited effect on the growth of primary rat HCC, but greatly decreased its metastatic potential. This is a very relevant finding because extrahepatic metastasis is clearly becoming a problem in the management of HCC patients, especially when attempts to control the primary tumor have been performed. Whereas beneficial effects of halofuginone on experimental tumor progression have been previously reported, all studies, with a single exception [9], dealt with grafted tumor cells in recipient animals. Our use of a highly relevant autochthonous model of liver carcinogenesis makes our results of special interest in a clinical perspective. Moreover, we show for the first time that halofuginone is able to dramatically reduce spontaneous metastasis. Although

Table 1. MMP activity in the liver.

	Tumors		Nontumoral part of the liver	
	Solvent (n = 4)	Halofuginone (n = 5)	Solvent (n = 4)	Halofuginone (n = 5)
MMP-9	1437 ± 160	534 ± 381*	1249 ± 267	134 ± 47*
Total MMP-2	444 ± 87	468 ± 215	415 ± 76	60 ± 21*
Active MMP-2 (%)	38.3 ± 2.3	15.0 ± 12.6*	28.8 ± 4.5	2.8 ± 6.2*

MMP activity was measured with gelatin zymography in liver samples from animals surviving up to week 24.
Values are in arbitrary units and are presented as mean ± 1 SD.
*P = .01, Mann-Whitney test.

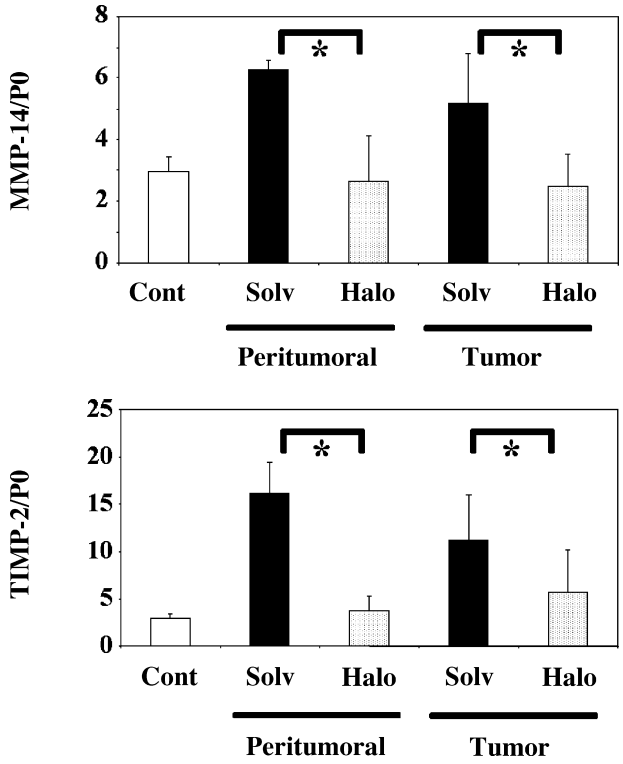

Figure 6. *The expression of transcripts of MMP-14 and TIMP-2 is reduced by halofuginone treatment. Transcripts of MMP-14 and TIMP-2 were assayed by quantitative PCR, and results were normalized according to the level of the P0 gene. Results are shown as mean ± SD. The upper panel shows MMP-14, and the bottom one shows TIMP-2. "Cont" refers to control animals that did not receive any carcinogens. "Solv" and "Halo" refer to animals bearing HCC that were treated with solvent or halofuginone, respectively. Measurements were made either in non-neoplastic parts of the liver or within tumors, as indicated. One-way analysis of variance showed that overall results differed significantly between groups (P < .006 for MMP-14 and P < .0003 for TIMP-2). Asterisks indicate significant differences between individual groups by post hoc Tukey's test (P < .01).*

an antimetastatic effect of halofuginone has been previously reported, it was in a much less relevant context of intravenous injections of a tumor cell line treated *in vitro* with halofuginone [15].

Our experiments pinpoint a possible mechanism by which halofuginone reduces tumor metastasis. Indeed, we found that halofuginone treatment had a profound effect on MMP expression and activity. On the first hand, halofuginone greatly reduced the expression of pro–MMP-9 both in tumors and in non-neoplastic parts of the liver. Although little active MMP-9 could be detected in control animals, none was seen under halofuginone treatment. In addition, halofuginone treatment led to a drastic decrease in the activation of MMP-2 in tumors and in nontumoral liver. It has already been shown that halofuginone could reduce MMP-2 expression likely through an inhibitory effect on the activity of the MMP-2 promoter [10,14,15]. Decreased MMP-9 expression has also been reported in cultured cells treated with halofuginone [10], although not *in vivo*. Mostly, the fact that halofuginone impedes MMP-2 activation has not been shown previously. Because only the cleaved, active form of MMP-2 is proteolytically active, this could be a very significant finding. The role of MMP-2 and MMP-9 in metastasis is largely substantiated (reviewed in Egeblad and Werb [23]). Animals with inactivation of either MMP-2 [24] or MMP-9 [25] are less susceptible to metastasis. In addition, selective inhibition of these two enzymes with a drug results in decreased metastasis [26]. Thus, the reduced activity of these two MMPs in liver tumors offers a plausible explanation for the beneficial effects of halofuginone on metastasis. Additional effects of halofuginone, notably on ECM remodeling, may also contribute to the antimetastatic effect.

In the final part of our study, we sought for an explanation to the decreased activation of MMP-2. MMP-2 is synthesized as an inactive zymogen form and must undergo a proteolytic cleavage of its prodomain to become catalytically active. Pro–MMP-2 is activated at the cell surface within a complex with membrane-associated MMP-14 (MT1-MMP) and TIMP-2 [21,22]. We found that halofuginone treatment greatly reduced the expression of the transcripts for these two proteins. It is likely that the resulting alteration in the stoichiometry of the complex may account for the decreased processing of pro–MMP-2. It is noteworthy that expression of MMP-14 and TIMP-2 is increased in human HCC [27] and that the amount of active MMP-2 is increased in these tumors [19]. It is thus likely that patients with HCC could benefit from halofuginone treatment. This could be of great significance because there are currently not many perspectives for these patients. In that respect, it is important to note that halofuginone tolerance is excellent in experimental animals and that human trials also point to good tolerance [28,29].

Acknowledgements

We are indebted to Mitsuru Futakuchi for help in setting up the rat HCC model and to Karin Halevy for critical reading of the manuscript. We thank the Comité de la Dordogne from the Ligue Nationale contre le Cancer, The Société Nationale Francaise de Gastroentérologie, and the Conseil Régional d'Aquitaine for supporting this project.

References

[1] Bosch FX, Ribes J, Diaz M, and Cleries R (2004). Primary liver cancer: worldwide incidence and trends. *Gastroenterology* **127,** S5–S16.

[2] Bruix J, Boix L, Sala M, and Llovet JM (2004). Focus on hepatocellular carcinoma. *Cancer Cell* **5,** 215–219.

[3] Shiina S, Teratani T, Obi S, Sato S, Tateishi R, Fujishima T, Ishikawa T, Koike Y, Yoshida H, Kawabe T, et al. (2005). A randomized controlled trial of radiofrequency ablation with ethanol injection for small hepatocellular carcinoma. *Gastroenterology* **129,** 122–130.

[4] Granot I, Bartov I, Plavnik I, Wax E, Hurwitz S, and Pines M (1991). Increased skin tearing in broilers and reduced collagen synthesis in skin *in vivo* and *in vitro* in response to the coccidiostat halofuginone. *Poult Sci* **70,** 1559–1563.

[5] Bruck R, Genina O, Aeed H, Alexiev R, Nagler A, Avni Y, and Pines M (2001). Halofuginone to prevent and treat thioacetamide-induced liver fibrosis in rats. *Hepatology* **33,** 379–386.

[6] Pines M, Knopov V, Genina O, Lavelin I, and Nagler A (1997). Halofuginone, a specific inhibitor of collagen type I synthesis, prevents dimethylnitrosamine-induced liver cirrhosis. *J Hepatol* **27,** 391–398.

[7] Levi-Schaffer F, Nagler A, Slavin S, Knopov V, and Pines M (1996). Inhibition of collagen synthesis and changes in skin morphology in

murine graft-*versus*-host disease and tight skin mice: effect of halofuginone. *J Invest Dermatol* **106,** 84–88.

[8] Nagler A, Firman N, Feferman R, Cotev S, Pines M, and Shoshan S (1996). Reduction in pulmonary fibrosis *in vivo* by halofuginone. *Am J Respir Crit Care Med* **154,** 1082–1086.

[9] Elkin M, Ariel I, Miao HQ, Nagler A, Pines M, de-Groot N, Hochberg A, and Vlodavsky I (1999). Inhibition of bladder carcinoma angiogenesis, stromal support, and tumor growth by halofuginone. *Cancer Res* **59,** 4111–4118.

[10] Gross DJ, Reibstein I, Weiss L, Slavin S, Dafni H, Neeman M, Pines M, and Nagler A (2003). Treatment with halofuginone results in marked growth inhibition of a von Hippel-Lindau pheochromocytoma *in vivo*. *Clin Cancer Res* **9,** 3788–3793.

[11] Gavish Z, Pinthus JH, Barak V, Ramon J, Nagler A, Eshhar Z, and Pines M (2002). Growth inhibition of prostate cancer xenografts by halofuginone. *Prostate* **51,** 73–83.

[12] Abramovitch R, Itzik A, Harel H, Nagler A, Vlodavsky I, and Siegal T (2004). Halofuginone inhibits angiogenesis and growth in implanted metastatic rat brain tumor model—an MRI study. *Neoplasia* **6,** 480–489.

[13] Pinthus JH, Sheffer Y, Nagler A, Fridman E, Mor Y, Genina O, and Pines M (2005). Inhibition of Wilms tumor xenograft progression by halofuginone is accompanied by activation of *WT-1* gene expression. *J Urol* **174,** 1527–1531.

[14] Elkin M, Miao HQ, Nagler A, Aingorn E, Reich R, Hemo I, Dou HL, Pines M, and Vlodavsky I (2000). Halofuginone: a potent inhibitor of critical steps in angiogenesis progression. *FASEB J* **14,** 2477–2485.

[15] Elkin M, Reich R, Nagler A, Aingorn E, Pines M, de-Groot N, Hochberg A, and Vlodavsky I (1999). Inhibition of matrix metalloproteinase-2 expression and bladder carcinoma metastasis by halofuginone. *Clin Cancer Res* **5,** 1982–1988.

[16] Nagler A, Ohana M, Shibolet O, Shapira MY, Alper R, Vlodavsky I, Pines M, and Ilan Y (2004). Suppression of hepatocellular carcinoma growth in mice by the alkaloid coccidiostat halofuginone. *Eur J Cancer* **40,** 1397–1403.

[17] Futakuchi M, Hirose M, Ogiso T, Kato K, Sano M, Ogawa K, and Shirai T (1999). Establishment of an *in vivo* highly metastatic rat hepatocellular carcinoma model. *Jpn J Cancer Res* **90,** 1196–1202.

[18] Clouzeau-Girard H, Guyot C, Combe C, Moronvalle-Halley V, Housset C, Lamireau T, Rosenbaum J, and Desmouliere A (2006). Effects of bile acids on biliary epithelial cell proliferation and portal fibroblast activation using rat liver slices. *Lab Invest* **86,** 275–285.

[19] Musso O, Théret N, Campion JP, Turlin B, Milani S, Grappone C, and Clément B (1997). *In situ* detection of matrix metalloproteinase-2 (MMP2) and the metalloproteinase inhibitor TIMP2 transcripts in human primary hepatocellular carcinoma and in liver metastasis. *J Hepatol* **26,** 593–605.

[20] Bieche I, Nogues C, Paradis V, Olivi M, Bedossa P, Lidereau R, and Vidaud M (2000). Quantitation of *hTERT* gene expression in sporadic breast tumors with a real-time reverse transcription–polymerase chain reaction assay. *Clin Cancer Res* **6,** 452–459.

[21] Butler GS, Butler MJ, Atkinson SJ, Will H, Tamura T, van Westrum SS, Crabbe T, Clements J, d'Ortho MP, and Murphy G (1998). The TIMP2 membrane type 1 metalloproteinase "receptor" regulates the concentration and efficient activation of progelatinase A. A kinetic study. *J Biol Chem* **273,** 871–880.

[22] Kinoshita T, Sato H, Okada A, Ohuchi E, Imai K, Okada Y, and Seiki M (1998). TIMP-2 promotes activation of progelatinase A by membrane-type 1 matrix metalloproteinase immobilized on agarose beads. *J Biol Chem* **273,** 16098–16103.

[23] Egeblad M and Werb Z (2002). New functions for the matrix metalloproteinases in cancer progression. *Nat Rev Cancer* **2,** 161–174.

[24] Itoh T, Tanioka M, Yoshida H, Yoshioka T, Nishimoto H, and Itohara S (1998). Reduced angiogenesis and tumor progression in gelatinase A–deficient mice. *Cancer Res* **58,** 1048–1051.

[25] Itoh T, Tanioka M, Matsuda H, Nishimoto H, Yoshioka T, Suzuki R, and Uehira M (1999). Experimental metastasis is suppressed in MMP-9–deficient mice. *Clin Exp Metastasis* **17,** 177–181.

[26] Kruger A, Arlt MJ, Gerg M, Kopitz C, Bernardo MM, Chang M, Mobashery S, and Fridman R (2005). Antimetastatic activity of a novel mechanism-based gelatinase inhibitor. *Cancer Res* **65,** 3523–3526.

[27] Theret N, Musso O, Turlin B, Lotrian D, Bioulac-Sage P, Campion JP, Boudjema K, and Clement B (2001). Increased extracellular matrix remodeling is associated with tumor progression in human hepatocellular carcinomas. *Hepatology* **34,** 82–88.

[28] Pines M, Snyder D, Yarkoni S, and Nagler A (2003). Halofuginone to treat fibrosis in chronic graft-*versus*-host disease and scleroderma. *Biol Blood Marrow Transplant* **9,** 417–425.

[29] Nativ O, Thorpe A, Laufer M, Matzkin H, Salzberg M, Yarkoni S, Dezube B, and Harris A (2004). Safety and tolerability of oral halofuginone hydrobromide in refractory recurrent transitional cell carcinoma of the bladder. *J Clin Oncol* **22,** 4757.